

## Impact Damage Sensing of Multiscale Composites Through Epoxy Matrix Containing Carbon Nanotubes

Luciana Arronche,<sup>1</sup> Valeria La Saponara,<sup>1</sup> Sertan Yesil,<sup>2</sup> Göknur Bayram<sup>3</sup>

<sup>1</sup>Department of Mechanical and Aerospace Engineering, University of California, Davis, California 95616, USA

<sup>2</sup>Department of Chemical Engineering, Kocaeli University, Kocaeli 41380, Turkey

<sup>3</sup>Department of Chemical Engineering, Middle East Technical University, Ankara 06800, Turkey

Correspondence to: V. La Saponara (E-mail: vlasaponara@ucdavis.edu)

**ABSTRACT:** Carbon nanotubes are used to provide increased electrical conductivity for polymer matrix materials, thus offering a method to monitor the structure's health. This work investigates the effect of impact damage on the electrical properties of multiscale composite samples, prepared with woven fiberglass reinforcement and epoxy resin modified with as-received multi-walled carbon nanotubes (MWCNTs). Moreover, this study addresses potential bias from manufacturing, and investigates the effectiveness of resistance measurements using two- and four-point probe methods. Transmission electron microscopy and static tensile tests results were used to evaluate, respectively, the dispersion of MWCNTs in the epoxy resin and the influence of the incorporation of these nanoparticles on the static tensile properties of the matrix, and interpret results from the resistance measurements on impacted specimens. In this study, the four-point probe method is shown to be much more repeatable and reliable than the two-point probe method. © 2012 Wiley Periodicals, Inc. *J. Appl. Polym. Sci.* 000: 000–000, 2012

**KEYWORDS:** composites; conducting polymers; sensors and actuators; mechanical properties

Received 14 May 2012; accepted 8 August 2012; published online

DOI: 10.1002/app.38448

### INTRODUCTION

Glass fiber-reinforced polymer (GFRP) composites have been largely employed in aircraft, naval and civil constructions, and wind turbine blades. Because of the complexity of their damage modes, it is necessary to achieve efficient ways of detecting their damage. Detection of damage through resistance changes requires in principle relatively simple measurements, with electrodes that can be attached *in situ* with minimal disruption of the surface, and with no major consequence on mechanical properties. Since glass fibers are not conductive on their own (in contrast with carbon fibers), a conductive polymer matrix is needed for this type of structural health monitoring. Because most polymer matrix materials are good insulators, this requires the incorporation of conductive nanoparticles. Carbon nanotubes (CNTs) are known for their exceptional mechanical and electrical properties, as showcased by Iijima.<sup>1</sup> They have been widely used to prepare electrically conductive composites and enhance their mechanical properties. On the other hand, CNTs' low dispersion capability and interfacial adhesion could originate weak composites.<sup>2</sup> Different factors affect the influence of the CNTs in the composite. For example, it was shown theoretically by Jiang et al.,<sup>3</sup> that the Young's modulus of a modified

polymer matrix increases up to 345 times if the distance between 30 nm diameter nanotubes is twice the minimum possible distance allowed by the van der Waals forces (i.e., 0.68 nm). On the other hand, the increase of Young's modulus is one order of magnitude less than in the previous case, if the 1 nm diameter nanotubes are distant 2.44 nm from each other. Therefore, it is important to understand and design CNTs in the composite, to obtain desired properties from them. Many methods are being employed in the literature to mechanically disperse the CNTs in epoxy resins, or chemically functionalize the surface of CNTs before incorporating them in epoxy.<sup>4,5</sup> However, there are surface treatments of CNTs that, depending on their concentrations in resin, cause lower or no conductivity of the resulting polymer when compared with untreated CNT-composites.<sup>6,7</sup> In one extensive review by Bauhofer and Kovacs,<sup>8</sup> it is shown that the conductivity of CNT-composites, where the CNTs were just mechanically mixed in epoxy, can be as high as that of chemically treated CNT-composites. In Ref. 8, the magnitudes of conductivity vary between  $1 \times 10^{-5}$  S/m and 10 S/m, and it is discussed that this property is influenced by several factors: type of CNTs (single, multi-walled), aspect ratio of CNTs, incorporation method, chemical treatment, etc.

In addition, the literature reports that epoxy matrices containing up to 0.5 wt % of treated or non-treated CNTs are a percolated conductive network,<sup>5,8–11</sup> and this allows damage detection by resistance changes. However, most of the work done seems to rely on a two-point probe measurement, a method that does not take into account contact resistance. In recent literature, damage due to quasi-static, fatigue tension, and impact loading was correlated to changes in resistance in fiberglass- and carbon-reinforced composites with a conductive polymer matrix, using two electrodes attached on the specimens.<sup>5,9,10,12–15</sup> In Ref. 16, an efficient way of detecting impact damage consisted of a surface-mounted grid to map damage. Although this was an efficient setup, the applicability to engineering parts may be limited, due to the electrodes complexity, data analysis, and increased weight.

Damage by impact may occur during the operational life of an engineering structure: it may be caused by bird strike, hail, debris, and tool drop during maintenance.<sup>17</sup> When a composite structure is impacted at low speeds (defined according to the interaction of the stress waves with the structure's boundaries), it may exhibit barely visible damage on the exposed surface, while the opposite surface may be fractured. Several techniques have been employed for impact damage detection, such as ultrasonic measurements (see e.g., Ref. 18), digital shearography, Electronic Speckle Pattern Interferometry, infrared thermography, e.g. Ref. 17. Impact damage detection by electrical resistance changes has also been investigated, although more work is needed: among the few available results, Yesil et al.<sup>5</sup> showed counter-intuitive results by two-point probe method (being investigated in this present work), Monti et al.<sup>14</sup> used low impact energy and two-point probe method, and Gao et al.<sup>15</sup> obtained a conductive matrix by adding a sizing agent containing CNTs, which by itself could affect results. Wen et al.<sup>19</sup> performed measurements in carbon fiber-reinforced composites not modified with CNTs, due to the inherent conductivity of these fibers.

The scope of the current work is to continue the study started in Ref. 5, and investigate the efficiency of electrical conductivity-based methods, to detect impact damage in conductive GFRP laminates. This could then be a viable structural health monitoring method for composite structures. Measurements using two- and four-point probe methods were compared to each other, to assess their reliability for health monitoring applications. Two-point probe and four-point probe measurements do not require a grid of probes for *in situ* measurements. Using a relatively simple and low-cost procedure to incorporate the multi-walled carbon nanotubes (MWCNTs) in epoxy matrix, conductive GFRP samples were manufactured for this study, without CNT functionalization. Moreover, a potential manufacturing bias was investigated. Results are interpreted with the use of transmission electron microscopy (TEM) and static tensile tests on the conductive epoxy matrix.

## EXPERIMENTAL METHODS

### Matrix Preparation

The materials used to prepare the conductive matrix were bisphenol A epoxy resin and hardener (117LV and 237 from Proset, Bay City, MI), and MWCNTs (NC7000 from Nanocyl,

Sambreville, Belgium) with 90% purity, a 9.5 nm average diameter, and a 1.5  $\mu\text{m}$  length. Epoxy matrix containing 0.5 wt % of as-received MWCNTs was prepared for this study. Based on our prior work, the percolation threshold of these as-received MWCNTs in the Proset resin is lower than 0.25 wt %.<sup>5</sup> In that work and in the current article, an amount of 0.5 wt % was utilized, for comparison with other studies in the literature.<sup>8–10,20</sup> The MWCNTs were dried for 24 h at 100°C prior to the matrix preparation, and then ground in a mortar. For the preparation of the impact and tensile test specimens' matrix, 1.95 g of MWCNTs and 200 mL of acetone were mixed and sonicated for 60 min at 25°C. After the sonication, 300 g of resin were added, and the solution was sonicated for 30 more minutes at the same temperature. The solvent was evaporated on a hot plate stirring non-stop at 200 rpm for 6 h at 50°C. This was followed by cooling in an ice bath for 40 min. The last step consisted of adding 90 g of hardener, and then mixing manually for 5 min. Degassing the mixture for 60 min was deemed necessary to remove its excess air.

### Dispersion Analysis and Tensile Tests

TEM analysis was made to evaluate the dispersion of the MWCNTs in the matrix material alone. Thin slices of matrix were cut from a matrix bulk and analyzed in a Philips CM12 microscope. A bright-field reflected light microscope Nikon Labophot 2A was also used to analyze the MWCNTs' dispersion. In particular, 5 mL of resin were extracted with a syringe during matrix preparation after one specific step (6 h on the hot plate, before the hardener was added), and inserted in a glass vial. The vial was observed for 2 days at room temperature, to study the precipitation of MWCNTs in epoxy.

Static tensile tests were performed to assess how the epoxy's tensile properties would be affected by the MWCNTs, compared to those of the neat resin. The prepared matrix/hardener mix was poured in a silicone rubber mold and cured for 15 h at room temperature, followed by 8 h at 82°C, as per manufacturer guidelines. The specimens' dimensions and tensile tests followed the ASTM D638-03 specifications, on an MTS 810 universal axial tester, loaded at 5 mm/min displacement control.

### Impact Tests

The materials used to manufacture the impact specimens consisted of the prepared matrix described in section "Matrix Preparation," and predominantly unidirectional woven fiberglass (type 7715 from Applied Vehicle Technology, Indianapolis, IN). The measured material properties for the lamina are longitudinal Young's modulus  $E_{11} = (37.6 \pm 2.22)$  GPa, major in-plane Poisson's ratio  $\nu_{12} = 0.254 \pm 0.0131$ , transverse Young's modulus  $E_{22} = (12.0 \pm 0.682)$  GPa, in-plane shear modulus  $G_{12} = (3.42 \pm 0.192)$  GPa. Three panels (herein indicated with "multi-scale composites" and consistently with the vocabulary used in the literature<sup>5,21,22</sup>) were manufactured by hand lay-up with stacking sequence  $[(0/90)_7,0]$ , and are named herein I, II, and III. Conventional vacuum-assisted resin transfer (VARTM) was not appropriate for the preparation of CNT-treated panels, because the epoxy with MWCNTs could not infiltrate the weave evenly, and the particles of MWCNTs appeared to be pushed away by the mere application of vacuum pressure. Additionally,

**Table I.** Impacted Specimens

Energy (J)	50	70
U group	I-3	III-4
	I-4	I-5
	I-1	II-2
T group	III-2	II-4
	II-3	II-1
	III-1	I-6

'U group' are specimens that were not turned over before impact, while 'T group' were turned before impact.

there was no functionalization process that would heighten the CNTs' adhesion to epoxy, and decrease the particle size of CNTs' agglomerates inside the matrix.

During the hand lay-up process, a metal plate ("base plate") was used at the bottom of the panel to keep the stack flat, and allow a uniform temperature during the curing cycle. Another heavier metal plate ("caul plate") was placed on the top of the lay-up for extra pressure during curing. The panels were cured under vacuum, respecting the manufacturer's curing cycle. Six specimens per panel were cut to dimensions 130 mm × 80 mm to fit inside the available impact fixture. The specimens were clamped along their 130 mm length.

Baseline specimens consisted of fiberglass infiltrated with neat epoxy, with the same stacking sequence, manufactured with two different processes: hand lay-up, for better comparison with the multiscale GFRP panels, and VARTM, which produces panels with higher apparent quality (less wrinkles and imperfections) than the panels prepared by hand lay-up. Impact tests demonstrated that the multiscale panels had actually higher resistance to impact in comparison with all baseline specimens, as will be discussed below. Hence, manufacturing by hand lay-up was not a liability from the standpoint of impact properties.

The impact tests were performed on a drop-weight machine (Instron Dynatup 9250G), according to ASTM D7136. Two sets of six multiscale specimens were impacted with 50 J and 70 J of energy, respectively. These energies were chosen because the prior study from our group<sup>5</sup> showed that these impact levels cause significant inelastic damage<sup>23</sup> (inelastic energy curves are discussed in more details in section "Impact Tests"). These impact levels thus allow an unambiguous assessment of this damage sensing method. The coupons selected from each batch were, respectively, Specimens 1, 3, 4, 5, and 6 from Batch I, Specimens 1, 2, 3, 4 from Batch II, and Specimens 1, 2, 4 from Batch III. The other specimens presented surface defects (wrinkling) and were not considered for further analysis. To study a possible manufacturing bias through the volume of the specimen, e.g., due to gravity effects during the processing of CNTs, three specimens from each set of six were randomly chosen and turned over. These specimens were therefore impacted on the surface that was initially in contact with the base plate during manufacturing. They are indicated herein as "T" specimens, to distinguish them from the specimens that were not turned before impact ("U" specimens), see Table I. Impact tests were also performed on baseline specimens, consisting of fiberglass

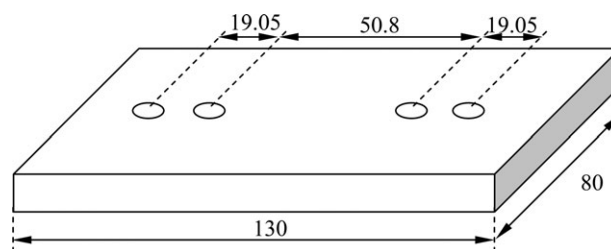


**Figure 1.** Impact test specimens dimensions and probes distances. All dimensions are in mm. Not to scale.

infiltrated with neat epoxy, with the same stacking sequence. Three specimens prepared by VARTM and two specimens prepared by hand lay-up were tested at each impact energy level.

### Electrical Resistance Measurements

Resistance was measured through two- and four-point probe methods. The total resistance measured by the easier-to-implement two-point probe technique is given by the sum of four terms: (a) wire and probe resistance, (b) the contact resistance between the probe and the material, (c) the resistance of the material itself, and (d) the spreading resistance, resulting from current transport between the probe and the material (see e.g., Ref. 24). The four-point probe method (also called Kelvin measurement) is a common technique that avoids errors caused by measurement of wire resistance, and thus is used in electrical circuits, for example in measurements of semiconductor material resistivity, or for finding poor connections or unexpected resistance in an electrical circuit.<sup>24–26</sup> Because of this theory, the four-point probe method was expected to have higher accuracy for multiscale composites as well, and the current study aimed at assessing and quantifying this accuracy.

Eight pieces of wire (DWG30 from Wire-Wrap<sup>®</sup>) with length 38.1 mm were attached, four on the top surface and four on the bottom surface of the specimens, with silver paste (number 8331-14 G from MGChemicals, Surrey, Canada), see Figure 1. Another function of the silver paste was to minimize the contact resistance between the sample surface and wires. There was no surface treatment prior to the wire attachment. A Keithley 199 multimeter measured resistance and voltage. The forces between the epoxy substrate and the silver paste are adhesive forces, since the matrix of the composite is a thermosetting material. After its 3D structure is formed upon curing, the material cannot be easily affected by the solvent contained in the silver

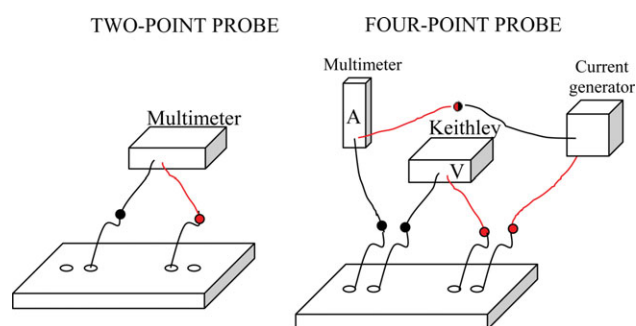


**Figure 2.** Two- and four-point probe measurements schemes. [Color figure can be viewed in the online issue, which is available at [wileyonlinelibrary.com](http://wileyonlinelibrary.com).]

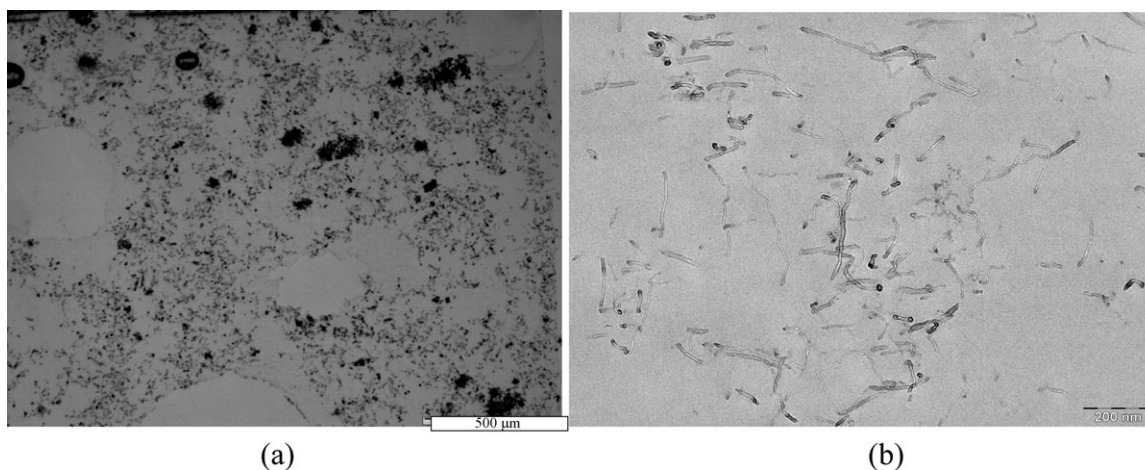


**Figure 3.** (a) optical microscopy showing clusters and dispersed MWCNTs and (b) TEM showing the dispersed MWCNTs.

paste. Another multimeter, Tektronix DMM916, was used to measure current. An amplifier/current generator with a 200 mA capacity (model A-303, A.A. Lab Systems, Ramat-Gan, Israel) was the current source. For the four-point probe method, a current of 200 mA was applied on the two outer probes, and the voltage was measured using the two inner probes (Figures 1 and 2). The resistance was calculated by Ohm's Law. In the two-point probe method, the resistance was measured directly on the two central probes (Figures 1 and 2).

For electrical measurements before and after impact, the "top" and "bottom" references were kept for data logging, resulting in a total of 12 measurements for each surface. The turned specimens "T" were turned back to the initial position for electrical measurements after impact: this means that the top surface had more visible damage compared to the bottom surface (the opposite for the unturned specimens "U").

## RESULTS AND DISCUSSION

### MWCNT/Epoxy Matrix

TEM and optical micrograph images are shown in Figure 3. It is well known that there is a difficulty of breaking the clusters

of CNTs for a better dispersion. The micrograph picture [Figure 3(a)] shows that there are still some clusters among the well-distributed MWCNTs. The TEM picture [Figure 3(b)] indicates that the MWCNTs not in clusters are well distributed. This distribution of the nanotubes in the matrix is accepted as reasonably homogeneous, and might be one reason for the material to become conductive. This is a result of the sonication and the stirring procedures applied during the preparation of the CNT/epoxy mixtures. Figure 4 shows pictures of the resin with CNTs right after preparation and after 1 day and 2 days in the glass vial, at room temperature. After 2 days, the vial was flipped and the picture was taken 1 h later. The resin does not flow. This all indicates that, at the end of the preparation of the conductive resin, the MWCNTs may not separate from the resin, as seen in Figure 4. However, it should be added that the actual curing of resin (CNT-treated and neat), once mixed with hardener, involves heating for several hours at 82°C, before it hardens. During this period, the viscosity of the resin will be lower. It may be possible that the CNTs may flow and deposit before the resin hardens, although this did not happen at room temperature in the resin alone. The effect of potential sedimentation of

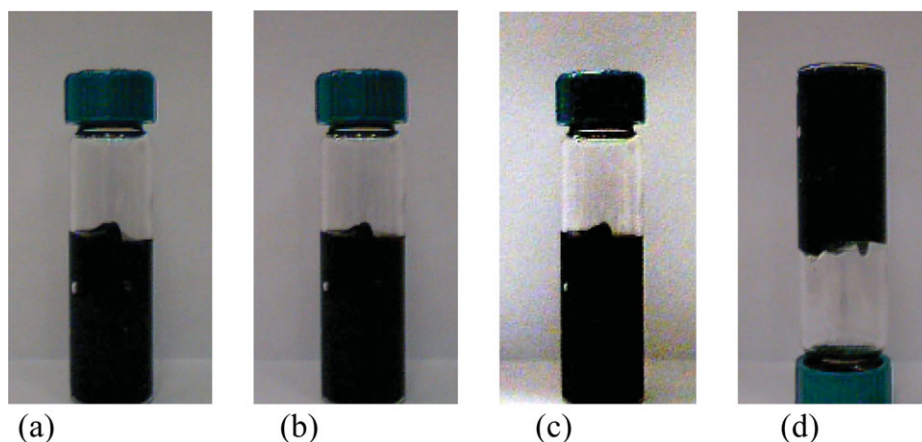


**Figure 4.** Vial with MWCNT/epoxy (no hardener): (a) right after preparation, (b) after 1 day, (c) after 2 days, (d) not flowing, after 1 h upside down. [Color figure can be viewed in the online issue, which is available at [wileyonlinelibrary.com](http://wileyonlinelibrary.com).]

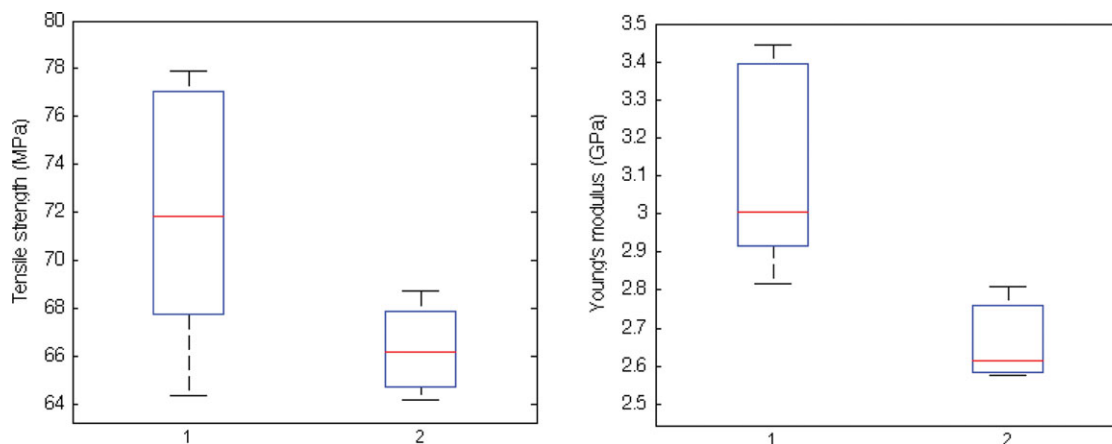


**Figure 5.** Tensile test results on epoxy/hardener. “1” is the neat epoxy, “2” the epoxy treated with MWCNTs. [Color figure can be viewed in the online issue, which is available at [wileyonlinelibrary.com](http://wileyonlinelibrary.com).]

CNTs was addressed in the study, as a possible manufacturing bias, and is discussed further below.

Static tensile tests were carried out, and the results were compared with previous results obtained by our group for neat epoxy (see Figure 5). The boxplot indicates that the presence of MWCNTs does not statistically influence the maximum tensile stress, while it decreases the longitudinal Young’s modulus. This could be due to interfacial slip of the MWCNTs in the matrix because of the lack of interfacial adhesion between the CNT and epoxy: in fact, the CNT surface is not chemically treated in this study, and functional groups are not present on the CNT surface, to improve the interfacial interactions during the application of the tensile load.<sup>27</sup> It is suggested that during the linear elastic behavior, interfacial slip of the MWCNTs occurs in the matrix, and the longitudinal strain is higher with a lower longitudinal stress component, compared to the neat epoxy. However, we should consider that the slip is limited, due to the size of the MWCNTs, and does not appear to affect the strength. This behavior is consistent with results available in the literature,<sup>28</sup> where two different types of CNTs were incorporated in

epoxy, and results for the elastic modulus were 10–19% lower compared with neat epoxy’s modulus. As shown in the following section, the GFRP specimens with treated resin (multiscale composites) had an enhanced impact resistance with respect to the baseline GFRP/epoxy specimens (GFRP samples with neat resin). Increased toughness is consistent with decreased stiffness.

### Impact Tests

Impact test results were interpreted with the use of inelastic energy curves, introduced by Rydin and Kharbari,<sup>23</sup> and similarly to Ref. 5. The impact tester’s acquisition software measures the load versus time data (see e.g., Figure 6), which is then used to calculate the impact energy curves (see e.g., Figure 7). Inelastic energies are built from the impact energy curves, and in particular the returned energy, which is equal to the maximum impact energy – final impact energy (note that the final impact energy is also the energy absorbed by the specimens, which is shown as an example in Figure 7). The returned energy is plotted against the nominal impact energy, to give the inelastic energy curves. Through the inelastic energy curves, it is possible to determine the impact energy levels at which the material

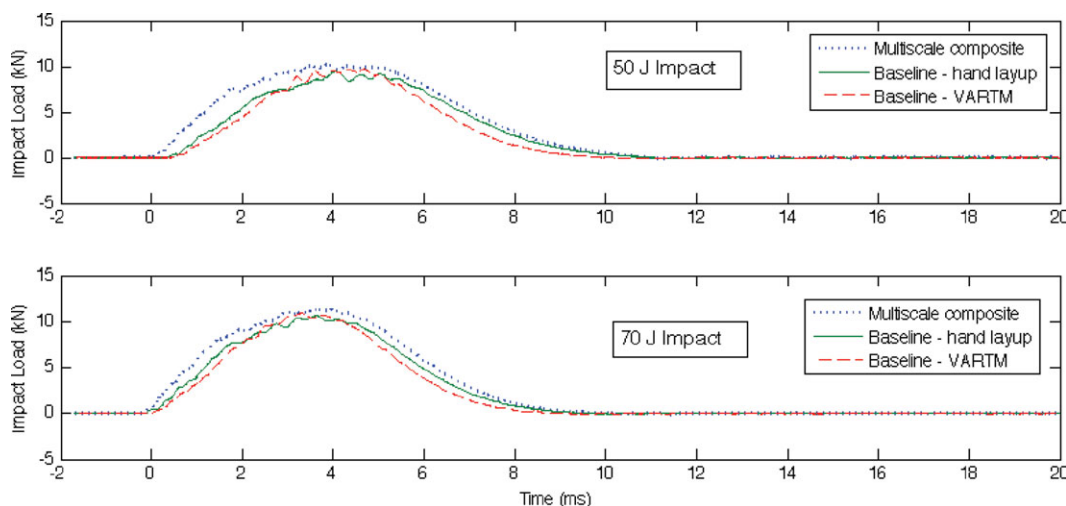


**Figure 6.** Representative load versus time curves for selected specimens under 50 J and 70 J impacts. The energy curves, for example Figure 7, are calculated based on the directly acquired load versus time data. [Color figure can be viewed in the online issue, which is available at [wileyonlinelibrary.com](http://wileyonlinelibrary.com).]

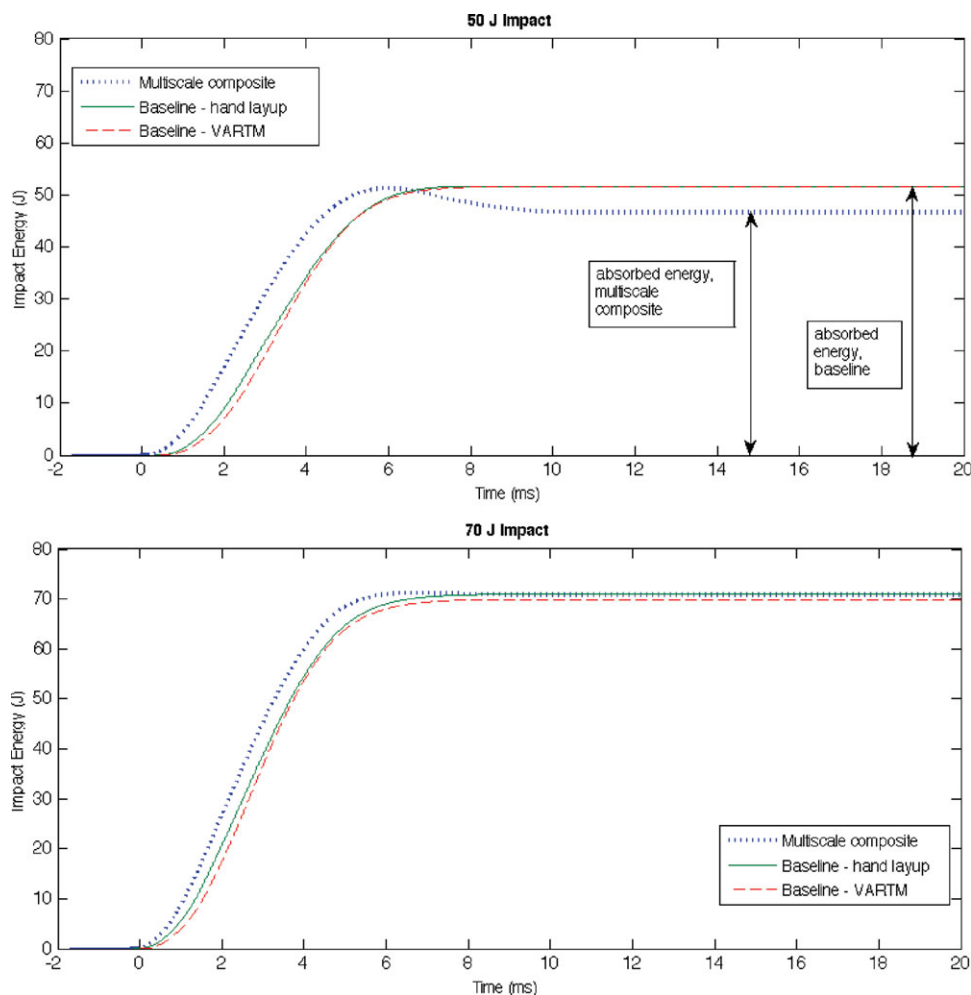


**Figure 7.** Representative energy versus time curves for selected specimens under 50 J and 70 J impacts, upon which the inelastic energy curves are calculated. [Color figure can be viewed in the online issue, which is available at [wileyonlinelibrary.com](http://wileyonlinelibrary.com).]

under study responds elastically or inelastically.<sup>23</sup> Thus, the amount of information provided is more complete with respect to the more conventionally used energy curves (such as Figure 7). Moreover, the impact levels causing significant damage may be computed without additional tests (e.g., on residual compressive strength). The enhancement of the multiscale composite's resistance under impact is observed because of the overall higher returned energy at both 50 J and 70 J energies, with respect to those of the baselines GFRP/epoxy specimens manufactured by hand lay-up and VARTM processes (Figures 6–8). Damage under 70 J impact was more significant, as indicated by the wider punctured area on the side opposite to impact. Hence, the higher extent of irreversible damage corresponds to a lower level of returned energy at 70 J with respect to a 50 J impact, and the error bars in Figure 8 show the variability of these results for all the specimens tested. It can be also observed that the manufacturing method for the baseline specimens does not affect significantly their response to impact (this is more evident in Figures 6 and 7 for a limited number of specimens).

The increased toughness of the multiscale composite may be due to the same interfacial slip of the MWCNTs in the matrix

that also affects the tensile properties (Figure 5). It is suggested that during impact loading, the slip of the MWCNTs in the matrix makes the material tougher, thus reducing the absorbed energy and resulting in an increase of output returned energy.<sup>27</sup> Moreover, MWCNTs present in the multiscale composite might decrease the crack formation and propagation during the impact test.<sup>29</sup> Figure 9 shows the surfaces of the impacted specimens: while there is barely visible damage on

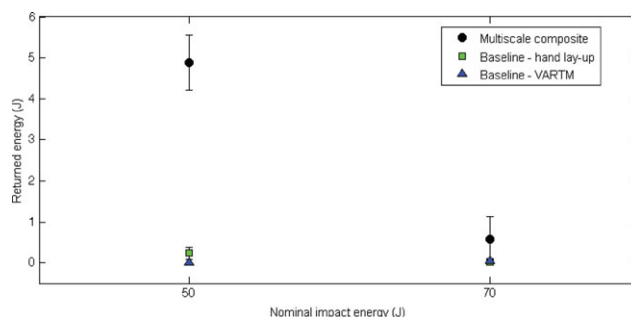


**Figure 8.** Inelastic energies with error bars, for all the specimens of this study, under 50 J and 70 J impacts. [Color figure can be viewed in the online issue, which is available at [wileyonlinelibrary.com](http://wileyonlinelibrary.com).]

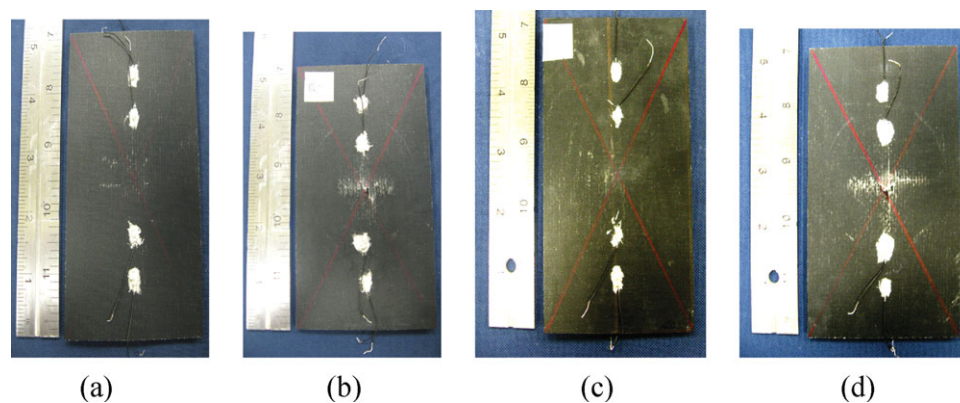


**Figure 9.** Under 50 J, (a) impacted surface and (b) back surface; under 70 J, (c) impacted surface and (d) back surface. [Color figure can be viewed in the online issue, which is available at [wileyonlinelibrary.com](http://wileyonlinelibrary.com).]

the impacted surfaces, the opposite sides of the specimens are clearly fractured, with a higher damage level for the 70 J, as expected. In summary, the incorporation of MWCNTs in epoxy through the solvent-assisted technique noted above seems to be beneficial for the impact resistance of the multiscale composites considered in this article. It is now discussed whether this process enables self-sensing of damage for these multiscale composites.

#### Electrical Resistance Measurements

Electrical conductivity results obtained in this study are consistent with the literature.<sup>16</sup> This may be explained by the homogeneous dispersion (section “MWCNT/epoxy Matrix”). Figure 10 gives conductivity data grouped by measurement method (two-point, four-point), before impact tests. The first and second boxes show that two-point measurements made on the bottom surface of the specimens have statistically higher variability when compared with the same type of measurements made on the top surface of the same specimens. The method used to attach the probes could cause this variability, due to the fact that the amount of silver paste on each probe was not precise and the shape of the probe was not easy to control. However, on the other hand, the four-point measurements show no statistical differences between top and bottom surfaces, and the inner probes used to measure the voltage were the same used for the two-point probe measurements. Higher conductivity is obtained by the four-point probe method, and the results’ variability is considerably lower when compared with the other method. Table II presents other statistical data not presented in the plots, e.g., mean, standard deviation, and coefficient of variation (“error” in Table II). In particular, the top conductivities measured by the two-point probe method have an error of 33%, while the four-point probe method is associated to an error of 14%. The bottom measurements show an even higher discrepancy, where the two-point and the four-point method give respectively an error of 51% and of 14%. Consequently, it is observed that the error for the four-point probe method is constant and lower with respect to the other method, in this study. This is consistent with the reputation of the four-point probe technique in the electrical circuits/semiconductors literature.<sup>25,26</sup>

For an improved statistical assessment, a One-Way Analysis of Variance (ANOVA) was computed, to find whether the null hypothesis  $H_0$  (no statistical difference in the population) or the alternative hypothesis  $H_1$  (statistical difference in the population) hold, with an  $\alpha$  risk (here, 0.05, that is 5%). A summary of ANOVA is given here.

ANOVA identifies the source of data variability as due to the variability between  $M$  treatments (given by the “factor  $A$  sum of squares,  $SSA$ ”), plus the variability of a total of  $N$  data within the  $M$  treatments (given by the “error sum of squares,  $SSE$ ”), see for example Ref. 30. These sums of squares are normalized appropriately (leading to “error mean squares,”  $MSE$ , and “error sum of squares,”  $SSE^{30}$ ). The ratio  $MSE/SSE$  follows an  $F$ -distribution (“ $F$ -statistics”). If such ratio is larger than a critical value of the  $F$ -distribution, then the null hypothesis may be rejected with a  $(1 - \alpha)$  confidence level. Alternatively, if the calculated “ $P$ -value” is larger than  $\alpha$  then the alternative hypothesis is rejected.

A key requisite for ANOVA is for the data to be normally distributed. The measurement data obtained with two-point probe method on the bottom surface of the specimens did not exhibit a normal distribution (as evaluated by the Lilliefors normality test). Therefore, this data was not included in the ANOVA. The ANOVA was applied to: Group 1, conductivity measurements before impact on the top surface, obtained by the two

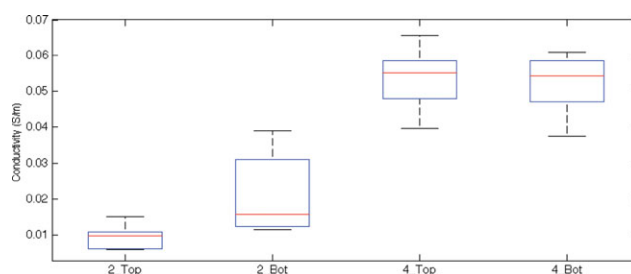


**Figure 10.** Top and bottom conductivities of the multiscale composites, measured with two-point probe method (first two boxes) and four-point probe method (last two boxes). “top,” “bot” indicate the surface where the measurement was made before impact. Each boxplot consists of 12 measurements. [Color figure can be viewed in the online issue, which is available at [wileyonlinelibrary.com](http://wileyonlinelibrary.com).]

**Table II.** Statistic Results of Specimens Conductivities [S/m] with Respect to Measurement Method (2-point, 4-point) and Surface Where the Measurement Was Made (“top,” “bottom”), Before Impact

	2-Point		4-Point	
	Top	Bottom	Top	Bottom
Mean	9.44 E-03	2.09 E-02	5.34 E-02	5.26 E-02
Standard deviation	3.13 E-03	1.07 E-02	7.56 E-03	7.60 E-03
Error (%)	33%	51%	14%	14%

**Table III.** ANOVA Analysis Between Two- and Four-Probe Methods, for Top Measurements Before Impact

Source	SS <sup>a</sup>	Df <sup>b</sup>	MS <sup>c</sup>	F	P-value
Columns	SSA = 0.01161	1	MSA = 0.01161	346.5056	5.94 E-15
Error	SSE = 0.000737	22	MSE = 3.35 E-05		
Total	SST = 0.012347	23			

<sup>a</sup>SS, sum of the squares, <sup>b</sup>Df, degree of freedom, <sup>c</sup>MS, mean square.

treatments two- and four-point probe methods (Table III); Group 2, conductivity measurements on top and bottom surfaces (now the two treatments) before impact, measured with four-point probe method (Table IV). The ANOVA tables, obtained by the commercial software MATLAB<sup>®</sup>, display: the source of variability (“columns” is the variability between treatments, and “error” is the variability within treatments), the sum of the squares (SSA for the “columns,” SSE for the “error”), degrees of freedom (Df = N - 1) and mean squares (MSA for the “columns,” MSE for the “error”), F-statistics and P-value. For the variance analysis of the first group (different methods, same surfaces), the P-value is much smaller than 0.05, which indicates highly significant difference, Table III. For Group 2, Table IV, the null hypothesis is true for the four-point probe method analyzed, because the P-value is higher than 0.05.

Figure 11 shows boxplots of conductivity data obtained before and after impact, grouped by measurement method, measured surface, and impact energy. Even though the impacted surface shows less damage than the surface opposite to the impact, there was no significant difference in conductivity before and after impact. For this reason, the data of “top” and “bottom” measurements were gathered in the same group for a comparison between methods.

From the plots, there is no easily defined pattern in the results obtained using the two-point probe method. The outcome of the four-point probe method, on the other hand, appears to be statistically the same. These results appear in contradiction with those by Gao et al.,<sup>15</sup> who indicated the difference between two-point

and four-point probe methods to be 1%. However, the latter article does not report the statistical analysis used for this assessment. Although the testing method and energy impact levels of our work and Ref. 15 are the same, the authors of Ref. 15 used a sizing agent containing CNTs, and thus the manufacturing process and the material are different from this current work. Another critical factor for the comparison with Ref. 15 is that key information is missing for the sake of a thorough comparison: the type of CNTs (multi-walled or single-walled) is unknown; the carbon nanotube content in the matrix is not reported, only the amount of sizing agent is mentioned. Therefore, while we report the apparently contradicting results of our work with Ref. 15, we are also unable to make any further comments because of the lack of sufficient information. On a positive note, the resistance changes of our composite panels under a 70 J impact are consistent with results showed in a plot in Ref. 15. In support of our results, the observed behavior of the measurements made with two- and four-point probe is similar to the outcome of Wang et al.<sup>31</sup> on carbon-fiber reinforced (CFRP) composites. To verify that the measurements from four-point probe are reasonably constant, additional analysis is given in Table V, which shows normalized resistivity changes before and after impact. The table shows that, for the four-point probe method, the normalized resistivity changes do not seem to depend on the surface where the measurement is carried out. Their means are <10% for the 50 J energy level, and ~15% for the 70 J level. It was expected that this difference would be higher than 15%: in fact, Monti et al.,<sup>14</sup> who also investigated impact damage in a similar composite, showed that composites impacted with a low energy level (11.7 J, barely visible damage) had a

**Table IV.** ANOVA Analysis Between Top and Bottom Measurements Made With Four-Probe Method, Before Impact

Source	SS <sup>a</sup>	Df <sup>b</sup>	MS <sup>c</sup>	F	P-value
Columns	SSA = 3.84 E-06	1	MSA = 3.84 E-06	0.066806	0.798449
Error	SSE = 0.001265	22	MSE = 5.75 E-05		
Total	SST = 0.001268	23			

<sup>a</sup>SS, sum of the squares, <sup>b</sup>Df, degree of freedom, <sup>c</sup>MS, mean square.



change in resistance of 7.7%. The specimens in this present work were instead completely punctured. Therefore, a 15% variation unfortunately may not be a significant variation of resistivity due to impact damage, when one considers that the manufacturing process involves several steps affected by scatter, e.g., hand lay-up. However, the increase of resistivity change between 50 J and 70 J is consistent with the expectation of more damage at 70 J and further disruption of the conductive network.

## CONCLUSIONS

GFRP laminates with a conductive matrix were tested under impact. The conductive epoxy matrix was obtained by incorporating 0.5 wt % of as-received MWCNTs in epoxy. TEM showed reasonably good dispersion of the MWCNTs in the matrix, testifying the effectiveness of the method used to incorporate the nanoparticles in the epoxy. Electrical resistance was measured before and after impact, to study the ability of the conductive matrix to sense damage. Measurements with two- and four-point probe methods were also assessed.

The four-point probe method proved to be considerably more reliable and repeatable than the two-point probe method. Due to the acceptable dispersion of MWCNTs in the epoxy matrix, no significant changes were supposed to be seen between the two locations (top surface, bottom surface) where the measurements were carried out. The four-point probe measurements reflect this occurrence, in contrast with the two-point probe method. The four-point probe method, by definition, is capable of eliminating/reducing contact resistances, and this leads to better results, as seen in this work. This conclusion is very important for any robust and repeatable assessment of resistance changes of nanocomposites. This article provides a well docu-

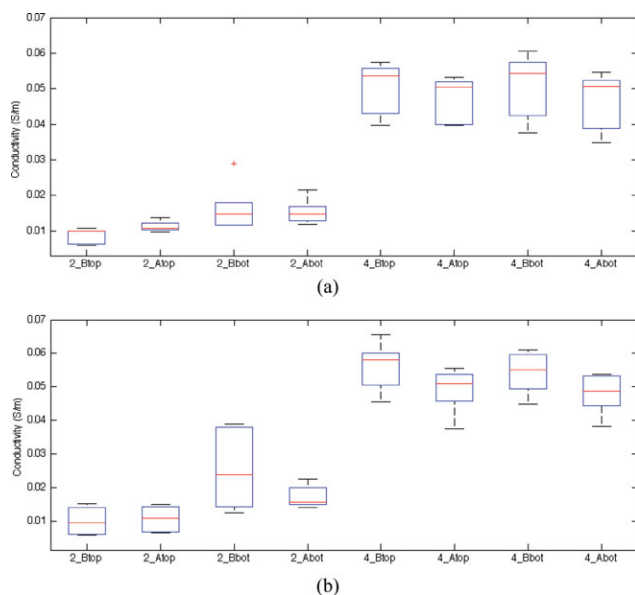


**Figure 11.** Conductivities of the multiscale composites before and after impact: (a) impacted with 50 J and (b) impacted with 70 J. “2” and “4” stand for two- and four-point probe methods, B and A for “Before impact” and “After impact,” and “top” and “bottom” are the surfaces where the measurements are made. [Color figure can be viewed in the online issue, which is available at [wileyonlinelibrary.com](http://wileyonlinelibrary.com).]

**Table V.** Normalized Resistivity, (After\_Impact–Before\_Impact)/Before\_Impact × 100, with its Individual Data and Mean ( $\mu$ ) and Standard Deviation ( $\sigma$ )

	2-Point		4-Point	
	Top	Bottom	Top	Bottom
50 J input impact energy				
U specimen				
I-1	-47	7	7	10
I-3	-43	-14	6	11
I-4	-28	-20	8	7
$\mu \pm \sigma$	$-39 \pm 10$	$-9 \pm 14$	$7 \pm 1$	$9 \pm 2$
T specimen				
II-3	-1	79	7	7
III-1	-7	-5	9	9
III-2	2	-2	-1	8
$\mu \pm \sigma$	$-2 \pm 5$	$24 \pm 48$	$5 \pm 5$	$8 \pm 1$
70 J input impact energy				
U specimen				
I-5	-29	-7	13	15
II-2	-10	140	11	11
III-4	5	2	21	18
$\mu \pm \sigma$	$-11 \pm 17$	$45 \pm 82$	$15 \pm 5$	$15 \pm 4$

Measurement types (two-point and four-point methods), surface where the measurement is made (‘top,’ ‘bottom’), and type of specimens (‘U,’ ‘T’) are given.

mented and statistically sound comparative analysis between two-point probe and four-point probe measurements on the same conductive specimens.

It was expected that the presence of a conductive matrix would be sufficient for damage detection using electrical measurements. However, resistivity changes did not appear to be very significant (up to 15%) for the impact energies of this work, even when measured using the four-point probe method, which means that it is likely not able to detect damage caused by low impact energies. This might be explained by the lack of functionalization of the MWCNTs in the epoxy. Consequently, functionalization is recommended.

## ACKNOWLEDGMENTS

The authors thank Mr. Bryan Loyola, Ph.D. student, UC Davis Advanced Composites Research, Engineering and Science (ACRES), for his assistance with the project, and Mr. Fred Hayes, Director of UC Davis Materials Science Central Facilities, for obtaining the TEM images. This paper is based upon work supported by the National Science Foundation to V. La Saponara (CA-REER Grant CMMI-0642814, and related IREE supplement).

## REFERENCES

- Iijima, S. *Nature* **1991**, *354*, 56.
- Yang, K.; Gu, M.; Guo, Y.; Pan, X.; Mu, G. *Carbon* **2009**, *47*, 1723.

3. Jiang, B.; Liu, C.; Zhang, C.; Liang, R.; Wang, B. *Compos. B* **2008**, *40*, 212.
4. Geng Y.; Liu, M. Y.; Li, J.; Shi, X. M.; Kim, J. K. *Compos. A* **2008**, *39*, 1876.
5. Yesil, S.; Winkelmann, C.; Bayram, G.; La Saponara, V. *Mater. Sci. Eng. A Struct.* **2010**, *527*, 7340.
6. Ma, M.; Wang, X.; *Mater. Chem. Phys.* **2009**, *116*, 191.
7. Ma, P. C.; Kim, J. K.; Tang, B. Z. *Compos. Sci. Technol.* **2007**, *67*, 2965.
8. Bauhofer, W.; Kovacs, J. Z. *Compos. Sci. Technol.* **2009**, *69*, 1486.
9. Kostopoulos, V.; Vavouliotis, A.; Karapappas P.; Tsotra, P.; Paipetis, A. *J. Intell. Mater. Syst. Struct.* **2009**, *20*, 1025.
10. Gao, L.; Thostenson, E. T.; Zhang, Z.; Byun, J.-H.; Chou, T.-W. *Philos. Mag. A* **2010**, *90*, 4085.
11. Grady, B. P. *Carbon Nanotube-Polymer Composites: Manufacture, Properties and Applications*; Wiley, Hoboken, NJ, **2011**.
12. Böger, L.; Wichmann, M. H. G.; Meyer, L. O.; Schulte, K. *Compos. Sci. Technol.* **2008**, *68*, 1886.
13. Thostenson, E. T.; Chou, T.-W. *Nanotechnology* **2008**, *19*, 215713 (6 p).
14. Monti, M.; Natali, M.; Petrucci, R.; Kenny, J. M.; Torre, L. *J. Appl. Polym. Sci.* **2011**, *122*, 2829.
15. Gao, L.; Chou, T.-W.; Thostenson, E. T.; Zhang, Z.; Coulaud, M. *Carbon* **2011**, *49*, 3382.
16. Proper, A.; Zhang, W.; Bartolucci, S.; Oberai, A. A.; Koratkar, N. *Nanosci. Nanotechnol. Lett.* **2009**, *1*, 3.
17. Gryzagoridis, J.; Findeis, D. *Insight* **2010**, *52*, 248.
18. Tsuda, H.; Toyama, N.; Urabe, K.; Takatsubo, J. *Smart Mater. Struct.* **2004**, *13*, 719.
19. Wen, J.; Xia, Z.; Choy, F. *Compos. B* **2011**, *42*, 77.
20. Kostopoulos, V.; Baltopoulos, A.; Karapappas, P.; Vavouliotis, A.; Paipetis, A. *Compos. Sci. Technol.* **2010**, *70*, 553.
21. Kim, M.; Park, Y.-B.; Okoli, O. I.; Zhang, C. *Compos. Sci. Technol.* **2009**, *69*, 335.
22. Bekyarova, E.; Thostenson, E. T.; Yu, A.; Kim, H.; Gao, J.; Tang, J.; Hahn, H. T.; Chou, T.-W.; Itkis, M. E.; Haddon, R.C. *Langmuir* **2007**, *23*, 3970.
23. Rydin, R.W.; Karbhari, V. M. *J. Reinf. Plast. Compos.* **1995**, *14*, 1175.
24. Doering, R.; Nishi, Y. *Handbook of Semiconductor Manufacturing Technology*; CRC Press: Boca Raton, **2008**.
25. Kuphaldt, T. R. *Lessons in Electric Circuit*, 5th ed., Vol. 1 DC. Available at [www.openbookproject.net/electricCircuits](http://www.openbookproject.net/electricCircuits), **2006**.
26. Schroder, D. K. *Semiconductor Material and Device Characterization*; Wiley: New York, **1998**.
27. Suhr, J.; Koratkar, N. A. *J. Mater. Sci.* **2008**, *43*, 4370.
28. Hernández-Pérez, A.; Avilés, F.; May-Pat, A.; Valadez-González, A.; Herrera-Franco, P. J.; Bartolo-Pérez, P. *Compos. Sci. Technol.* **2008**, *68*, 1422.
29. Meincke, O.; Kaempfer, D.; Weickmann, H.; Friedrich, C.; Vathauer, M.; Warth, H. *Polymer* **2004**, *45*, 739.
30. Tamhane, A. C.; Dunlop, D. D. *Statistics and Data Analysis from Elementary to Intermediate*; Prentice Hall, Inc.: New Jersey (US), **2000**.
31. Wang, S.; Wang, D.; Chung, D. D. L.; Chung, J. H. *J. Mater. Sci.* **2006**, *41*, 2281.